scientific reports

Check for updates

OPEN

Pharmacological applications and plant stimulation under sea water stress of biosynthesis bimetallic ZnO/MgO NPs

Samy Selim[1]✉, Mohammed S. Almuhayawi[2], Mohammed H. Alruhaili[2,3], Muyassar K. Tarabulsi[4], Amna A. Saddiq[5], Mohammed Yagoub Mohammed Elamir[1], Mohamed A. Amin[6]✉ & Soad K. Al Jaouni[7]

The uniqueness and novelty of this study lies in the ability of *Mentha longifolia* leaves extract (MLLE) to synthesize bimetallic NPs (NPs) of zinc oxide and magnesium oxide as nanocomposite (ZnO/MgO NPs) for the first time. Medicinal plants extracts are a more environmentally friendly method of creating NPs than physical or chemical methods. The specific objectives of the research were employed this nanocomposite compared to plant extract as antibacterial, anti-diabetic, antioxidant agents. Also, the possibility of using this nanocomposite as plant stimulator for reducing saline water stress on economic plants to cope with the scarcity of freshwater in the agricultural sector. In comparison to nanocomposite, MLLE exhibited high inhibition zones 28 ± 0.1, 26 ± 0.2, 26 ± 0.1, 25 ± 0.2, 25 ± 0.1 and 24 ± 0.1 mm in medium inoculated by *E. faecalis*, *E. coli*, *S. typh*, *M. circinelloid C. albicans*, and *S. aureus*, respectively. It was shown from the DPPH data that ZnO/MgO NPs' IC_{50} value (52.55 ± 0.98 µg/mL) was lower than the extract's (299.27 ± 1.59 µg/mL) when compared to ascorbic (195.15 ± 1.63 µg/mL). Compared to acarbose, ZnO/MgO NPs exhibited superior activity against α-Amylase inhibition percentage, as evidenced by their IC_{50} value of 117.02 ± 0.56 µg/mL. In contrast to ZnO/MgO NPs, acarbose had a lower IC_{50} value of 22.15 ± 0.76 µg/mL. ZnO/MgO NPs were added to the soil cultivated by cucumber plants (A pots experiment) at quantities of 0, 200, and 400 mg/kg. Bimetallic ZnO/MgO NPs, particularly at 200 ppm, improved the shoot and root lengths and fresh weight of shoot, but they also seemed to reduce the level stress indicator of MDA, H_2O_2, and antioxidant enzymes (peroxidase and polyphenol oxidase). As a result, ZnO/MgO NPs may be employed as a unique approach to boost plant growth under salinity stress.

Keywords ZnO/MgO NPs, Antimicrobial, Green synthesis, Application, Sea water stress

Nowadays, the chemical, mechanical, pharmaceutical, agricultural and food processing industries view nanotechnology as a validated technology with a variety of uses[1–5]. Numerous methods, such as mechanical milling, microwave-assisted synthesis, homogeneous precipitation have been planned for the creation of NPs (NPs)[6], but in general, they endanger the environment. Green synthesis of NPs is an easy-to-manage and design substitute for these techniques[7]. Green synthesis provides a sustainable, ecofriendly and economical substitute for conventional nanoparticle synthesis techniques, which call for the use of dangerous chemicals and excessive energy usage. This method makes use of biologically active substances and natural resources that can function as capping, stabilizing, or reducing agents[8–10]. In order to achieve the maximum biological performance of agrochemicals without overdosing, nano-fertilizers may offer a targeted/controlled release of such chemicals.

[1]Department of Clinical Laboratory Sciences, College of Applied Medical Sciences, Jouf University, 72388 Sakaka, Saudi Arabia. [2]Department of Clinical Microbiology and Immunology, Faculty of Medicine, King Abdulaziz University, 21589 Jeddah, Saudi Arabia. [3]Special Infectious Agents Unit, King Fahad Medical Research Center, King Abdulaziz University, Jeddah, Saudi Arabia. [4]Department of Basic Medical Sciences, College of Medicine, University of Jeddah, Jeddah, Saudi Arabia. [5]Department of Biological Sciences, College of Science, University of Jeddah, Jeddah, Saudi Arabia. [6]Botany and Microbiology Department, Faculty of Science, Al-Azhar University, Cairo, Egypt. [7]Department of Hematology/Oncology, Yousef Abdulatif Jameel Scientific Chair of Prophetic Medicine Application, Faculty of Medicine, King Abdulaziz University, 21589 Jeddah, Saudi Arabia. ✉email: sabdulsalam@ju.edu.sa; mamin7780@azhar.edu.eg

Environmental pollutants may be found and eliminated using nanosensors and nanoremediation techniques. However, physico-chemical characteristics that impact the toxicity of nanomaterials, potential interactions with co-formulants in the agro-system, and stressors should be evaluated[11]. Antimicrobial resistance has become a global health concern due to antibiotic abuse, overuse, and misuse, necessitating quick, innovative, and long-lasting solutions. An environmentally benign, economical, sustainable, and renewable solution to this pressing issue is the use of bio-nanomaterials as antibiotic allies. These biomaterials' use of green precursors (biowaste, plant extracts, essential oils, microorganisms, and agricultural residue) and fabrication processes that reduce their cyto/environmental toxicity and show cost-effective manufacturing. The improved biocompatibility and nanoscale dimensions of bio-nanomaterials offer special advantages in the battle against antibiotic resistance[12,13]. Also, through the development of immunity, early detection, nanotherapeutics, and tailored drug delivery systems, biogenic nanometals can help manage cancer[14]. In our study we used *Mentha longifolia* extract as reducing agent to prepare bimetallic NPs, because it has a unique, fragrant scent and is used as a nervous system laxative, to treatment various digestive disorders, and to promote the growth and function of salivary glands and digestive enzymes. Based it is being a natural source for developing drugs. It is also used in toothpastes because of its ability to fight tooth decay-causing bacteria and because its strong smell helps open the respiratory passages, which helps relieve coughing and expel sputum[15].

Metal oxide NPs of magnesium oxide (MgO) and zinc oxide (ZnO) exhibit a wide range of characteristics, like little dielectric constant, high chemical stability, and photostability. These features have been used thus far in a widespread of industrial and scientific utilizations, comprising catalysis and the development of among antibacterial and antimicrobial substances. In general, ZnO is thought to be more potent than magnesium oxide at eliminating bacteria[16]. It is possible to create a wide variety of additional zinc oxide (ZnO) nanostructures, including spheres, rods, flowers, disks, walls, and more. However, because of its many uses, such as biosensors, gas sensors, therapeutic cancer cell killing, biosensors and biological pollutants, nanoflowers and nanowires have drawn special attention[17,18].

The capacity of ZnO to liberate toxic ions of zinc to bacteria is the reason for this. These ions have the ability to interfere with bacterial cell membranes, alter biological functions, and result in cell death. In addition, mild inhibition zones show that MgO and ZnO NPs have activity against growth of several bacteria[19]. Additional uses for MgO NPs have been documented, including anti-inflammatory, anti-cancer, antioxidant, and anti-diabetic effects[20,21].

The application of NPs in agriculture reduces the need for excessive chemical fertilizers and significantly improves plant growth and seed germination across a variety of plant species[22]. Global climate change and ongoing chemical application are already posing a threat to agricultural sustainability. These elements have had a significant impact on the productivity, growth, and nutritional state of different crops. Consequently, plants' susceptibility to stress can be increased either directly or indirectly by the unintentional discharge of nanostructures into surrounding environment including air, and water, as well as soil. However, further research is required to fully understand how NPs affect plants[23]. There is proof that the precursors of seed dressing compounds, which boost crop growth and productivity, are nanomaterials[24]. Treatment of mustard seeds by different doses of MgO NPs prior to planting, improved the plants' vegetative characteristics, yield traits, photosynthetic pigment, biomass, carbohydrate content, and superoxide dismutase, catalase activity[25]. ZnO NPs minimize drought-stressed cucumber development when applied at doses ranged from 25 to 100 mg/L, they significantly increased biomass, photosynthetic pigments, and growth under normal condition, while lessening the effects of drought[26]. Mg is a macronutrient element that is involved in plant progress as well as in physiological pathways. A lack of Mg may lead to a decline in the Calvin cycle's efficiency, a decrease in the usage of reductive power (Nicotinamide adenine dinucleotide phosphate), and an oversaturation of the photosynthetic electron transport system, which would inhibit plant development and lower pod production[27]. Zn is a vital mineral element for plant development that affects many aspects of plant growth in both positive and negative ways. It is a part of many biochemical processes, including enzyme synthesis, protein synthesis, chlorophyll synthesis, and metabolic turnover[28]. However, plants suffer when they lack zinc, so using zinc oxide nanofertilizer (ZnO NF) in place of ZnO NPs is an interesting idea that is currently being researched[29].

In the current study *Cucumis sativus* L. was used as a model of cultivar cultivate at stress condition of salinity. *C. sativus* L. is ranked fourth among the major vegetable crops, following *Brassica oleracea*, *Allim cepa*, and *Solanum lycopersicum* and is frequently consumed raw or combined with other foods[30]. Over 33 and 20% of irrigated agricultural soil and cultivated soil, respectively suffer from salinity worldwide[31]. Osmotic and ionic imbalance induces a number of modifications in the systems involved in development, leading to oxidative stress[32]. Furthermore, plants have a variety of defense mechanisms, such as ionic homeostasis, antioxidant activities, and the activation of a large number of associated with stress genes[33]. This investigation aimed to: investigate the ability of *M. longifolia* leaves extract to synthesize bimetallic zinc/magnesium oxide NPs ZnO/MgO NPs, to reduce the harmful influence of sea water on morphological and biochemical traits of cucumber plants. In addition to being used as an antioxidant, anti-diabetic and antibacterial agents.

Materials and methods

Aqueous extract of *Mentha longifolia* leaves preparation

Young, healthy, and fresh *M. longifolia* leaves were gathered from botanical garden of faculty of science-al-Azhar university-Nasr city-Cairo-Egypt. The plant has been identified by taxonomist Prof. Abdo A. Hamed of the Botany and Microbiology Department, Faculty of Science, Al-Azhar University, Egypt. A plant specimen was deposited in the local botanical herbarium of Botany and Microbiology Department, Faculty of Science, Al-Azhar University, Egypt. Any solid dust particles were then washed away using double-distilled water and flowing tap water; and then dried (in dark at 30 °C) for two weeks. To obtain a powder the dried plant leaves, a coffee grinder was utilized. After that, they were heated in sterile distilled H_2O at a ratio of one/one hundred

(w/v) for 45 min at 60 °C. The obtained filtrate was stored at 4 °C in a closed container until they were used to create NPs.

Zinc and magnesium bimetal NPs preparation

A bimetallic of ZnO/MgO NPs was made using an easy, environmentally friendly procedure. 250 ml of an aqueous extract of *Mentha longifolia* leaves, 10 mM zinc chloride, and 0.5 M magnesium chloride were combined, and the mixture was constantly agitated at 70 °C for 3 h. Upon evaporating the synthesized solution, the residue was collected and then cleaned with deionized water and alcohol to remove any remaining contaminants. To obtain the reddish-brown powder needed for the following procedures, the collected residue was annealed for 2 h at 200 °C. It was then stored in a falcon tube.

Zn and mg oxide NPs characterization

ZnO/MgO NPs' 200–800 nm spectra were examined using a UV–VIS Spectrophotometer (SYSTRONICS). The NPs' size and shape were examined via transmission electron microscopy (TEM). Using energy dispersive X-ray (EDX) examination, the various chemical components of the NPs were identified. FTIR (Fourier transform infrared) spectra were used to further establish the chemical makeup of the NPs.

Microorganisms inhibition test

The agar well diffusion approaches were utilized to evaluate the antibacterial properties of *M. longifolia* leaf extract and *M. longifolia* leaf extract mediated Zn/MgNPs against a variety of bacterial and fungal species, such as *Escherichia coli* (ATCC 8739), *Enterococcus faecalis* (ATCC 10541), *Staphylococcus aureus* (ATCC 6538), *Salmonella typhi* (ATCC 6539), and *Candida albicans* (ATCC 10221), besides *Mucor circinelloid* (AUMMC 11656). To do this, the bacterial strains were adjusted to 106 CFU/mL in turbidity and then evenly distributed across plates containing Mueller-Hinton agar employing a sterile cotton swab. Then, 100 µL of *M. longifolia* leaf extract and *M. longifolia* leaf extract-mediated Zn/Mg NPs at 0.5 mg/mL concentrations were applied to each of the 6-mm-diameter wells. After incubating at 37 °C for 24 h, the widths of the clear (inhibition) area were determined to evaluate the activity of examined materials. Standard drugs including gentamycin and nystatin were applied for positive control[34].

Testing of ZnO/MgO NPs mediated by *M. longifolia* leaves at 1.95 to 250 µg/mL against tested bacteria and *C. albicans* was done to determine minimum inhibitory concentration (MIC) employing the broth microdilution method in 96-well microplates. The twofold serial dilution was made with Mueller Hinton broth (MHB). The microbial suspension, containing 2×10^8 CFU/mL, was added to 100 µL of the microplate wells that held the twofold serial dilutions of the examined materials solution in the MHB. This study used McFarland Standard No. 0.5, whose cell density (2×10^8 CFU/ml) was found using the absorbance at 600 nm. To determine the MIC, the biological substance that inhibited bacterial growth was measured at its lowest concentration following a 24-h aerobic incubation with 5% CO_2 at 37 °C. As positive and negative controls, respectively, the bacteria put to the MHB devoid of testing samples and the growth media free of bacteria were identified. The turbidity-free blood agar medium was added to ten microliters of the microbial suspensions in the wells in order to calculate the MBC. The combination was then allowed to develop sufficiently before being kept in an incubator at 37 °C. The MBC was described as the least dose at which 99.9% of the original inoculum was eliminated at each interval of contact[35].

α-Amylase assessment

The α-amylase inhibition experiment was carried out using the 3, 5-dinitrosalicylic acid (DNSA) method[36], where different concentrations of the investigated materials (acarbose and NPs) (1000 to 1.95 µg mL^{-1}) were prepared in separate test tubes with 0.02 M phosphate buffer (pH = 6.9). 500 µL of α-amylase was then added, and the tubes were incubated for 10 min at 37 °C. Each tube was then filled with 500 µL of 1% starch solution, and it was incubated for 10 min. The reaction was then stopped by adding 1 mL of 3,5-dinitrosalicylic acid (DNA) to each tube. The tubes were then cooled and finished with 10 mL of dH_2O after being incubated for 15 min at 60 °C in a water bath. The color absorbance, measured spectrophotometrically at 540 nm, shows the percentages of α-amylase inhibition that were assessed by this equation

$$\text{inhibition percentages} = \frac{Ac - At}{Ac} \times 100$$

α-Glucosidase assessment

The approach outlined by Pistia Brueggeman and Hollingsworth[37] was slightly modified to evaluate the potential of plant extracts to inhibit α-glucosidase. Where, in a test tube with 150 µL of sodium phosphate buffer (0.1 M) and 1 U of the enzyme α-glucosidase, 100 µL of each concentration of the compounds under test (acarbose, NPs) were added. The combination was then incubated for 10 min at 37 °C. The test tube was then filled with 50 µL of p-Nitrophenyl-α-D-glucopyranoside (2 mM) and incubated for 20 min at 35 ± 2 °C. 50 µL of sodium carbonate (0.1 M) was added to halt the reaction, and the absorbance of the color that resulted was measured at 405 nm before using previous equation we can determine the percentages of α-glucosidase inhibition.

DPPH radical scavenging technique to assess antioxidant activity

The ability of *M. longifolia* leaf extract and *M. longifolia* leaf extract mediated ZnO/MgO NPs to scavenge free radicals was evaluated using 1, 1-diphenyl-2-picryl hydrazyl (DPPH) at various concentrations (3.9, 7.8, 15.62, 31.25, 62.5, 125, 250, 500, and 1000 µg/mL). The absorbance at 517 nm was measured using a spectrophotometer (UV-VIS Milton Roy). With ascorbic acid acting as the reference standard component[38].

Total antioxidant capacity assay (TAC)

For each sample (0.5 mg/mL), one milliliter was mixed with three milliliters of the reagent solution (0.6 M H_2SO_4, 28 mM sodium phosphate (NaH_2PO_4), and 4 mM ammonium molybdate). Within the blank solution, there were just 4 milliliters of reagent solution. At 95 °C, the mixtures were incubated for 150 min. The mixture was allowed to cool to ambient temperature before absorbance was recorded at 630 nm employing a microtiter plate reader (Biotek ELX800; Biotek, Winooski, VT, USA)[39].

Ferric reducing antioxidant power (FRAP) examine

This study investigated the influence of solvent polarity on the total reducing power of the *M. longifolia* leaf extract and *M. longifolia* leaf extract mediated ZnO/MgO NPs using potassium ferricyanide and trichloroacetic acid[40]. With further adjustments created especially for the microplate approach. After this point, total reducing power (TRP) will be utilized to represent ferric reducing antioxidant power (FRAP). 40 milliliters of the sample, 50 milliliters of 10% trichloroacetic acid, 50 milliliters of 1% potassium ferricyanide ($K_3Fe(CN)_6$), and 50 milliliters of sodium phosphate dihydrate ($Na_2HPO_4{\cdot}2H_2O$) buffer were put into labeled Eppendorf tubes. Centrifuging the mixture at 3000 rpm for 10 min was the process. Six hundred and sixty-six milliliters of the supernatant from every sample and seventy-five milliliters of ferric chloride ($FeCl_3$, 1%) were placed onto 96-well plates. At 630 nm, measurements were taken using a Microtek ELX800 microtiter plate reader (Biotek, Winooski, VT, USA). There were two controls used: a positive control with 1 mg/mL of ascorbic acid and a negative control with DMSO. Ascorbic acid equivalent (AAE), or milligrams per milligram of extract, was used to report the results.

A pot experiment

The seeds of cucumber (*Cucumis sativus*) were bought from the Agricultural Research Center of the Ministry of Agriculture in the Egyptian province of Giza. We planted 25 cm-diameter pots with 4.0 kg of clay soil inside to start the cucumber seeds. Four groups of pots were created, each of which represented a distinct kind of treatment. (1) Tape water (Control); (2) Sea water 35% (pH: 7.85, salinity percent: 41.57, TSS: 16 (mg/L) BOD 3.34 (mg/L) irrigation; (3) Sea water irrigation 35% + 200 mg/kg Zn/Mg nanoparticle/kg soil; (4) Sea water irrigation 35% + 400 mg Zn/Mg nanoparticle /kg soil. The developing plants received as-needed irrigation with 35% of Sea water but, control group irrigated with tape water. At 40 days next planting, samples of plant from the different treatments and the control were taken for estimated growth traits, pigments contents, H_2O_2, MDA, and antioxidants enzymes.

Determination of metabolic contents in shoots

Enzymatic antioxidant activity assays

As stated by Mukherjee and Choudhuri[41], the following procedure was used to extract the enzymes: Following the homogenization of 2 g plant terminal buds and the 1st and 2nd young leaves using 10 mL of phosphate buffer pH 6.8 (0.1 M), the mixture was spun for 20 min at 20,000 rpm in a refrigerated centrifuge at 2 °C. It was found that the enzymes were present in the clear supernatant, which served as the source of the enzyme.

Polyphenol oxidase (PPO)

We measured the polyphenol oxidase activity with the methods outlined by Kar and Mishra[42]. The substrate was a sodium acetate buffer (pH 5.0) involving 0.1 M catechol. The measurements were taken at 395 nm, and the reaction was permitted to run for 60 min at 30 °C (Ultrospec 2000). Alterations in optical density min^{-1} g^{-1} fresh mass (FM) were used to indicate polyphenoloxidase activity.

The enzyme peroxidase (POX)

The peroxidase activity was measured using the subsequent procedure, which was adopted from Bergmeyer et al.[43]: A pH 7.0 phosphate buffer was mixed with the reaction mixture, which included 5.8 milliliters of a 50 mL, 2 mL of 20 mM H2O2, and 0.2 mL of enzyme extract. Employing a UV-spectrophotomer, the absorbance increased as the pyrogallol was recorded spectrophotometrically within 60 s at 470 nm and 25 °C.

Assay for lipid peroxidation

The amount of malondialdehyde (MDA) in fresh leaves was used to quantify lipid peroxidation. This was accomplished by grounding samples of the leaves (0.2 g) and adding 2 mL of 5% trichloroacetic acid (w/v). After that, the homogenate was centrifuged (10 min/4°C/10,000 rpm). The mixture was centrifuged for 10 min at 4 °C and 10,000 rpm after adding 2 mL of 0.67% thiobarbituric acid (w/v) to 2 mL of the supernatant. The mixture was then preserved in a boiling water bath for 30 min. The absorbance of the supernatant was then measured at 450, 532, and 600 nm. After that, the MDA content was determined using the following formula:

$$MDA = 6.45 \times (A532 - A600) - (0.56 \times A450).$$

Levels of lipid peroxidation were expressed as micromoles of MDA/g of fresh mass, or μmol g^{-1} FM[44].

The hydrogen peroxide level was calculated subsequently a reaction with potassium iodide (KI), according to Sergiev et al.[45]. The reaction mixture composed of 0.5 M KI, leaf extract, and 2.5 mM K-phosphate buffer (pH 7.0). The reaction mixture was kept in the dark for 60 min. The quantity of H_2O_2 was recorded at 390 nm using spectrophotometry and a standard curve created with solution H_2O_2.

Statistical analysis

Microsoft Excel version 365 and Minitab version 19 were the computer programs used for the statistical computations at 0.05 level of probability. Analysis of variance was performed using the One-way ANOVA and

Post hoc-Tukey's test for quantitative data with a parametric distribution. The allowable margin of error was set at 5%, while the confidence interval was set at 95%.

Results and discussion

Characterization of bimetallic ZnO/MgO NPs

Ecofriendly method in the present investigation was employed to prepare bimetallic Zn/Mg NPs via aqueous extract of *M. longifolia* leaves for the first time applying. ZnO/MgO NPs displayed an absorption maximum at 360 nm in the UV-Vis spectrophotometric analysis (Fig. 1A), which was in line with previous studies that revealed ZnO/MgO NPs' characteristic peak to be among 350 and 360 nm[46]. The size the NPs was reported via TEM (transmission electron microscopy), which ranged in nano scale, were depicted by the HRTEM image. In TEM image (Fig. 1B), exhibiting both spherical and hexagonal shapes. Additionally, the ZnO/MgO NPs' surface capping was disclosed by the FTIR results (Fig. 1C).

ZnO/MgO NPs had an FTIR spectrum with a range of 500–4000 cm^{-1}. The composite had a variety of functional groups and metal-oxide bonds. An important vibration band at 435.63, and 629.79 cm^{-1} was

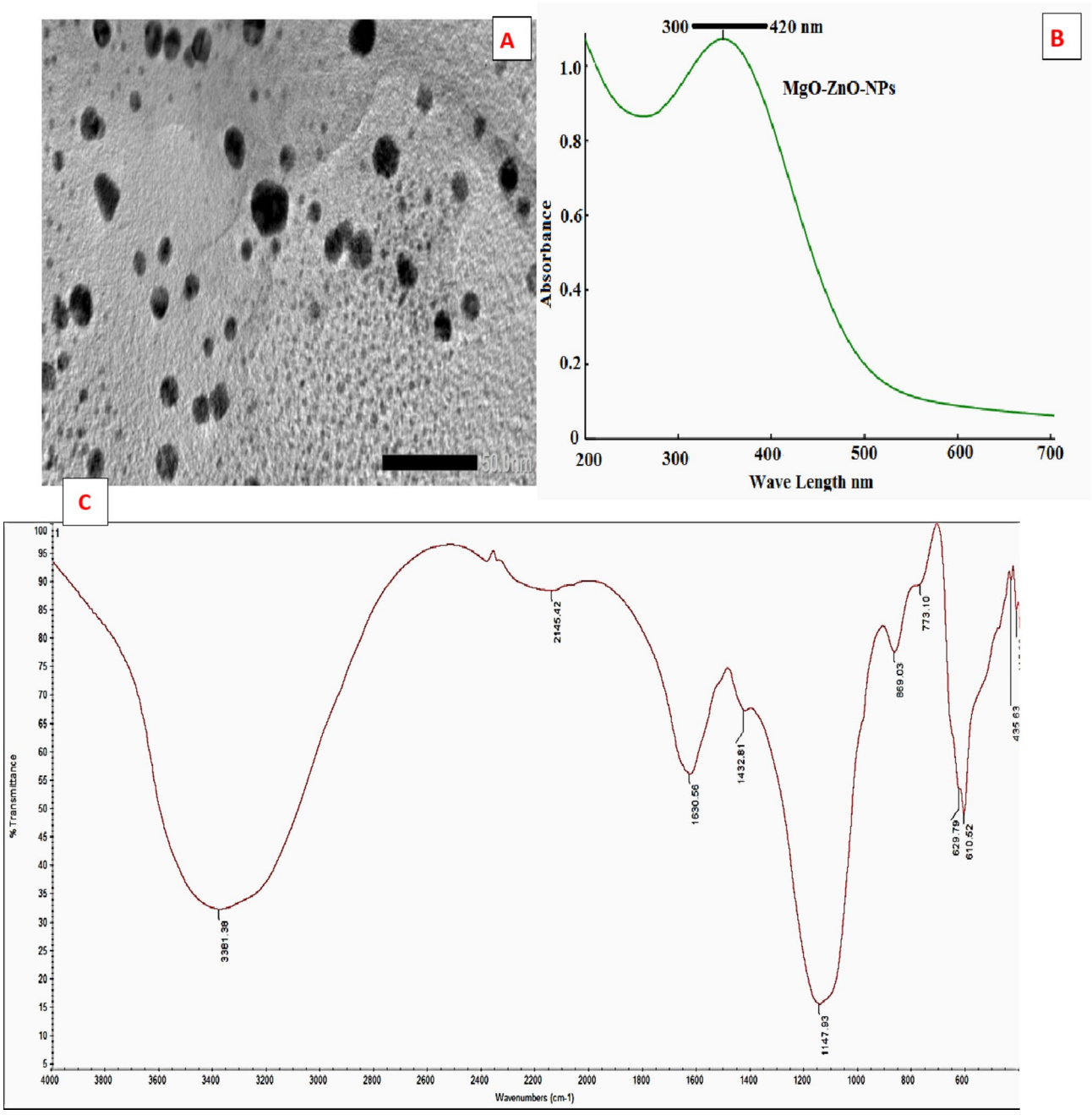

Fig. 1. (**A**) HR-TEM appearance, (**B**) UV spectroscopy and (**C**) FTIR of the *Mentha longifolia*-synthesized bimetallic ZnO-MgO NPs.

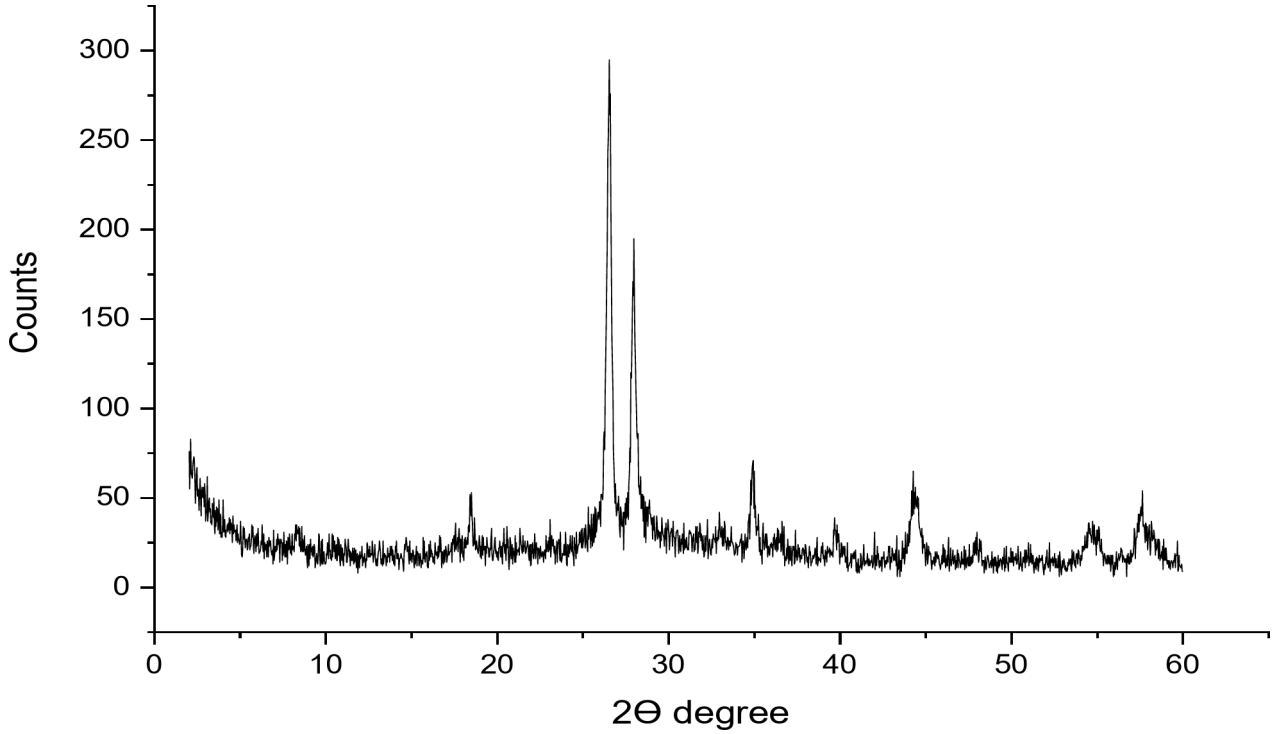

Fig. 2. XRD spectroscopy of the *M. longifolia*-synthesized bimetallic ZnO-MgO NPs.

Tested microorganisms	Inhibition zones (mm)			Negative control (DMSO)	HSD
	Extract	ZnO@MgO NPs	Positive control (Gentamycin/Nystatin)		
E. faecalis	28 ± 0.1a	26 ± 0.2b	24 ± 0.1c	0.0	1.35
S. aureus	24 ± 0.1a	21 ± 0.3b	25 ± 0.1a	0.0	1.16
E.coli	26 ± 0.2a	22 ± 0.1b	21 ± 0.2b	0.0	1.42
S. typhi	26 ± 0.1a	20 ± 0.1b	18 ± 0.2c	0.0	0.95
C. albicans	25 ± 0.1a	24 ± 0.2b	24 ± 0.3b	0.0	0.33
M. circinelloid	25 ± 0.2b	15 ± 0.1c	27 ± 0.1a	0.0	0.32

Table 1. Antimicrobial potential of extract, ZnO@MgO NPs, positive control and negative control. The data shows means ± standard error ($n = 3$). According to Tukey's test (HSD), significant differences ($P \leq 0.05$) are indicated by different lowercase letters in the same species within a column.

identified as the ZnO bond's typical stretching mode[47]. Peaks at 869.03 and 610.52 cm^{-1} may be significant for the magnesium oxide NPs' distinctive absorbance at this particular wavelength. It strengthens the Mg-O bonding and facilitates the creation of MgO-NPs[48]. The O-H stretching peak in the ZnO/MgO NPs FTIR spectrum is responsible for the bands that appear at 3381 cm^{-1}, while the C=C stretching peaks appear at 1630 cm^{-1}, the C-C stretching peak at 1432 cm^{-1}, the C-O stretching peak at 1147 cm^{-1}, the 869 cm^{-1} and 773 cm^{-1} bands are caused by the =C-H bending. FTIR spectrum band peak analysis, which is consistent with the previously published work, confirmed that ZnO/MgO NPs have bioactive functional groups that support stability and antibacterial action[49].

The XRD pattern of the generated ZnO/MgO NPs is shown in Fig. 2. The standard JCPDS card Numbers 00-005-0094 and 00-012-0643 complement the diffraction peaks at 2Θ = 18.4654°, 26.5682°, 27.9478°, 34.9089°, 39.7598°, 44.3585°, 48.0023°, 54.5345°, and 57.5919° that were emphasized in the XRD data of the generated bimetallic ZnO-MgO NPs. The XRD pattern indicates that the product is highly crystalline due to the presence of sharp peaks. The cause of a few significant peaks could be instrumental broadening[50,51].

Antimicrobial activity of ZnO/MgO NPs

From the obtained results, the created bimetallic NPs (ZnO/MgO NPs) showed antimicrobial activities but it was less than the extract. Extract caused inhibition zones were 28 ± 0.1, 24 ± 0.1, 26 ± 0.2, 26 ± 0.1, 25 ± 0.1 and 25 ± 0.2 mm while 26 ± 0.2, 21 ± 0.3, 22 ± 0.1, 20 ± 0.1, 24 ± 0.2, and 15 ± 0.1 mm against *E. faecalis*, *S. aureus*, *E. coli*, *S. typhi*, *C. albicans* and *M. circinelloid*, correspondingly compared to control (Table 1; Fig. 3). The extract's MIC and MBC against the studied bacteria were lower than those of ZnO/MgO NPs. Less % between the values

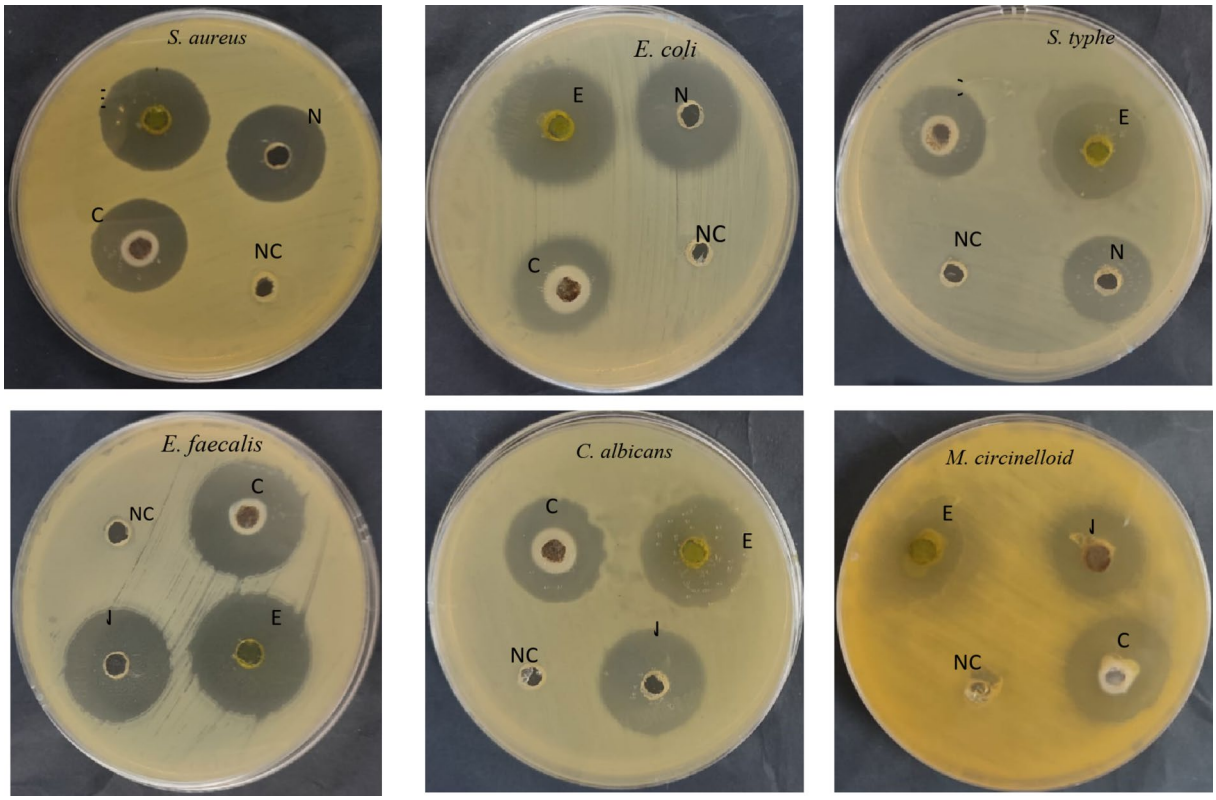

Fig. 3. Antimicrobial activity of ZnO@MgO NPs (N), extract (E), and antibiotic/antifungal as a positive control (C) against microorganisms under test. The impact of DMSO as a negative control (NC) with a well-defined zone.

Tested microorganisms	MIC (µg/mL)			MBC (µg/mL)			MBC/MIC Index		
	Extract	ZnO@MgO NPs	HSD	Extract	ZnO@MgO NPs	HSD	Extract	ZnO@MgO NPs	HSD
E. faecalis	7.8 ± 2.3b	15.62 ± 1.25a	4.21	7.8 ± 2.21b	62.5 ± 3.25a	5.15	1 ± 0.65b	4 ± 0.45a	1.25
S. aureus	62.5 ± 2.3b	125 ± 3.21a	6.32	125 ± 2.25b	250 ± 3.45a	5.32	2 ± 1.32a	2 ± 1.24a	0.32
E.coli	15.62 ± 3.4b	62.5 ± 2.15a	4.36	31.25 ± 2.1b	125 ± 1.89a	6.56	2 ± 0.51a	2 ± 0.45a	0.21
S. typhi	15.62 ± 3.2b	125 ± 4.32a	6.54	15.62 ± 1.2b	125 ± 2.54a	4.02	1 ± 0.32a	1 ± 0.41a	1.05
C. albicans	7.8 ± 0.45a	7.8 ± 0.32a	0.21	7.8 ± 0.09a	7.8 ± 0.05a	0.16	1 ± 0.15a	1 ± 0.21a	0.56
M. circinelloid	15.62 ± 3.2b	500 ± 4.21a	6.65	62.5	–	2.54	4 ± 0.58	–	1.32

Table 2. MIC and MBC of Extract and ZnO@MgO NPs. The data shows means ± standard error ($n = 3$). According to Tukey's test (HSD), significant differences ($P \leq 0.05$) are indicated by different lowercase letters in the same species within a column.

of MIC of the extract and ZnO/MgO NPs was observed, respectively in the case of *E. faecalis* (7.8 and 15.62 µg/mL), followed by *S. aureus* (62.5 and 125 µg/mL), followed by *E. coli* (15.62 and 62.5 µg/mL), followed by *S. typhi* (15.62 and 125 µg/mL). In the same context, Less % between the values of MBC of the extract and ZnO/MgO NPs was observed, respectively in the case of *S. aureus* (125 and 250 µg/mL), followed by *E. coli* (31.25 and 125 µg/mL), followed by *E. faecalis* (7.8 and 62.5 µg/mL), and *S. typhi* (15.62 and 125 µg/mL). MIC and MFC values of the extract were the same MIC and MFC values of ZnO/MgO NPs (Table 2). In recent study, ZnO NPs exhibited antimicrobial activity towards *Bacillus subtilis*, *Staphylococcus aureus*, *Pseudomonas aeruginosa*, *Escherichia coli*, *Candida albicans*, and *Salmonella typhi*[2], these microorganisms were also inhibited by the phytosynthesized ZnO NPs[21] but the *Mucor circinelloide* was not inhibited however in the current study it was inhibited by ZnO/MgO NPs. This may be due to the presence of bimetal NPs or may role of phytomediator of ZnO/MgO NPs synthesis. So, Al-Rajhi et al.[52] found that CuONPs promoted the efficacy of ZnONPs against different microbiology. Regarding the antimicrobial activity, our results were agreement with Al-Rajhi et al.[53], where *M. pulegium* exhibited inhibitory activity versus *B. subtilis*, *E. coli*, *S. aureus*, and *C. albicans* with inhibition zones 27, 26, 19, and 25 mm, respectively due to the existence of isochiapin B and neophytadiene. Other study documented the bactericidal potential of *M. pulegium* extract Ceyhan-Güvensen and Keskin[54] due to its high content neophytadiene content. All values of *M. pulegium* extract were lower than that of ZnO/MgO NPs in all

Dose (µg/mL)	DPPH scavenging %			HSD
	Ascorbic acid	Extract	ZnO@MgO NPs	
1000	98.2 ± 2.52a	78.7 ± 3.21c	93.2 ± 1.65b	3.32
500	94.4 ± 1.65a	71.9 ± 2.36c	86.7 ± 3.54b	3.65
250	92.4 ± 2.65a	64.5 ± 1.87c	80.1 ± 3.65b	4.89
125	88.5 ± 2.12a	57.6 ± 1.45c	73.0 ± 3.45b	3.21
62.50	82.2 ± 1.58a	51.0 ± 2.51c	66.6 ± 3.12b	4.21
31.25	75.8 ± 2.15a	43.9 ± 2.36c	59.6 ± 4.32b	6.25
15.63	69.5 ± 2.54a	37.0 ± 1.02c	53.4 ± 2.64b	4.21
7.81	62.3 ± 3.54a	29.6 ± 2.98c	47.3 ± 1.41b	5.48
3.90	54.3 ± 2.45a	22.7 ± 1.65c	41.1 ± 3.45b	3.87
1.95	46.6 ± 2.85a	16.3 ± 1.45c	33.7 ± 2.67b	4.21
0.0	0.0 ± 0.0	0.0 ± 0.0	0.0 ± 0.0	0.0 ± 0.0
IC_{50} µg/mL	195.15 ± 1.63b	299.27 ± 1.59a	52.55 ± 0.98c	8.25

Table 3. DPPH scavenging % of extract, ZnO@MgO NPs and ascorbic acid. The data shows means ± standard error ($n = 3$). According to Tukey's test (HSD), significant differences ($P \leq 0.05$) are indicated by different lowercase letters in the same species within a column.

Treatment	TAC (equivalent (AAE) µg/mg of extract)	FRAP (equivalent (AAE) µg/mg of extract)
ZnO@MgO NPs	195.8 ± 0.5b	294.0 ± 1.6a
Extract	318.5 ± 0.7a	298.5 ± 1.0b
HSD	1.21	3.54

Table 4. The extract's antioxidant capacity and ZnO@MgO NPs via ferric reducing antioxidant power and total antioxidant capacity. The data shows means ± standard error ($n = 3$). According to Tukey's test (HSD), significant differences ($P \leq 0.05$) are indicated by different lowercase letters in the same species within a column.

cases of tested bacteria except *C. albicans*, while MBC values were less than that of ZnO/MgO NPs in all cases of microorganisms. Seghir et al.[19] tested the MgO and ZnO NPs separately against various bacteria including *Listeria innocua*, *B. subtilis*, *S. aureus*, *Salmonella typhimurium* and *P. aeruginosa*, who also found ZnO NPs were more effective than MgO NPs.

Antioxidant activity of ZnO/MgO NPs

According to Tukey's test at $P \leq 0.05$, both plant extract and ZnO/MgO NPs and positive control (ascorbic acid) showed significant differences of antioxidant activity. DPPH scavenging % encourages with increasing the concentration as visualized in Table 3. But as noticed from the results the IC_{50} value of ZnO/MgO NPs (52.55 ± 0.98 µg/mL) was less than that of the extract (299.27 ± 1.59 µg/mL) compared to ascorbic (195.15 ± 1.63 µg/mL). Al-Rajhi et al.[53] mentioned that *M. pulegium* extract possess antioxidant activity with IC_{50} value 18 µg/mL. According to the results of the current study, the presence of various phenols and flavonoids is linked to the primary sources of antioxidant activity. In the present research, TAC and FRAP confirmed the antioxidant potential of both ZnO/MgO NPs and extract (Table 4). Strong (318.5 ± 0.7) TAC activity of extract was detected while ZnO/MgO NPs reflected (12.5 µg/mL, µg AAE/mg) moderate TAC activity (195.8 ± 0.5 µg, AAE/mg). The antioxidant potential of ZnO/MgO NPs NPs and extract was further assayed by FRAP. FRAP experiment indicated the slight increase in the antioxidant potential of extract (298.5 ± 1.0 µg AAE/mg) compared to ZnO/MgO NPs (294.0 ± 1.6 µg AAE/mg). According to Baali et al.[55], numerous methods, such as oxygen radical absorbance capacity, ferric reducing antioxidant power, and trolox equivalent antioxidant capacity, have been used to report the antioxidant activity of *M. pulegium*.

Anti-diabetic activity of ZnO/MgO NPs

By preventing α-Amylase and α-Glucosidase in vitro, plant extract and ZnO/MgO NPs have the potential to prevent diabetes (Table 5). The degree of inhibition of α-Amylase and α-Glucosidase increased as the concentration of plant extract and ZnO/MgO NPs increased up to 1000 µg/mL, but at different rates. A promising result were observed using ZnO/MgO NPs with IC_{50} 6.5 ± 0.36 µg/mL against α-Amylase inhibition % and 120.76 ± 1.19 µg/mL against α-Glucosidase inhibition % compared with IC_{50} of extract against α-Amylase inhibition % (260.05 ± 1.09 µg/mL) and against α-Glucosidase inhibition % (291.22 ± 60 µg/mL). Moreover, According to statistical analysis at $P \leq 0.05$, both plant extract and ZnO/MgO NPs and positive control (Acarbose) showed significant differences of α-Amylase and α-Glucosidase inhibition % but, ZnO/MgO NPs showed better activity against α-Amylase inhibition % than Acarbose which reflected IC_{50} value of 117.02 ± 0.56 µg/mL. While

Concentration (µg/mL)	α-Amylase inhibition %			HSD	α-Glucosidase inhibition %			HSD
	Acarbose	Extract	ZnO@MgO NPs		Acarbose	Extract	ZnO@MgO NPs	
1000	87.9 ± 1.32b	78.7 ± 2.15c	95.0 ± 1.69a	3.32	89.8 ± 1.10a	75.1 ± 0.89c	84.6 ± 1.21b	3.32
500	81.7 ± 0.98b	72.6 ± 0.65c	90.6 ± 0.78a	3.21	84.0 ± 0.56a	69.3 ± 0.78c	78.5 ± 0.89b	2.21
250	75.1 ± 1.65b	66.1 ± 1.89c	84.0 ± 0.87a	2.87	78.4 ± 0.25a	63.2 ± 0.36c	72.6 ± 0.42b	1.23
125	68.7 ± 0.98b	59.9 ± 1.20c	78.2 ± 0.68a	2.21	73.0 ± 0.15a	57.8 ± 0.36c	67.4 ± 0.21b	0.96
62.50	62.3 ± 1.02b	53.7 ± 0.89c	71.8 ± 0.32a	3.32	67.1 ± 0.85a	51.8 ± 0.36c	61.7 ± 0.58b	2.10
31.25	56.3 ± 0.87b	47.5 ± 1.02c	65.5 ± 0.68a	2.23	61.6 ± 1.02a	45.6 ± 0.95c	55.2 ± 0.80b	3.21
15.63	49.8 ± 0.25b	40.4 ± 0.32c	58.6 ± 0.58a	1.21	56.6 ± 0.52a	39.6 ± 0.45c	48.2 ± 0.42b	1.35
7.81	42.9 ± 0.09b	34.4 ± 0.25c	47.1 ± 0.16a	0.65	50.3 ± 0.25a	34.2 ± 0.36c	44.6 ± 0.19b	0.85
3.90	36.2 ± 0.89b	27.6 ± 1.03c	40.6 ± 0.75a	2.36	44.0 ± 1.09a	28.4 ± 0.87c	38.8 ± 0.65b	2.32
1.95	30.0 ± 1.05b	21.4 ± 1.16c	34.2 ± 0.69a	3.26	38.1 ± 0.82a	23.2 ± 1.02c	33.6 ± 0.86b	2.48
0.00	0.0 ± 0.0	0.0 ± 0.0c	0.0 ± 0.0	00	0.0 ± 0.0	0.0 ± 0.0	0.0 ± 0.0	00
IC_{50} µg/mL	117.02 ± 0.56b	260.05 ± 1.09a	6.5 ± 0.36c	6.32	22.15 ± 0.76c	291.22 ± 60a	120.76 ± 1.19b	4.36

Table 5. Activity inhibition of α-amylase and α-glucosidase by Extract, ZnO@MgO NPs, and acarbose. The data shows means ± standard error ($n = 3$). According to Tukey's test (HSD), significant differences ($P \leq 0.05$) are indicated by different lowercase letters in the same species within a column.

Treatments	Shoot lengths (cm)	Root lengths (cm)	Fresh weight of shoot (g)
Control	24.17 ± 6.83 a	5.77 ± 1.97a	9.56 ± 6.22a
Control saline	16.17 ± 3.33 b	3.33 ± 0.57b	2.87 ± 1.85b
Saline + 200 mg ZnO@MgO NPs	21.33 ± 3.21a	6.83 ± 3.69a	8.76 ± 1.33a
Saline + 400 mg ZnO@MgO NPs	18.66 ± 1.53ab	5 ± 1a	3.66 ± 0.76b
HSD	4.17	2.77	3.79

Table 6. Growth traits of Cucumber under various treatments. The data shows means ± standard error ($n = 3$). According to Tukey's test (HSD), significant differences ($P \leq 0.05$) are indicated by different lowercase letters in the same species within a column. The standard deviation of the means plus the mean of three replicates make up each number. Values of the same letter in the same column do not differ significantly; nevertheless, post hoc Tukey's test results at $P < 0.05$ show significant differences between distinct lower-case letters in the same column.

acarbose reflected less IC_{50} value of 22.15 ± 0.76 µg/mL than ZnO/MgO NPs. Anti-diabetic potential of ZnO NPs via inhibiting α-glucosidase and α-amylase enzymes was reported[56].

Morphological and biochemical traits of cucumber treated by of ZnO/MgO NPs

One important and harmful abiotic element that prevents plants from developing and producing as much is salinity[57]. Bimetallic ZnO/MgO NPs at 200 and 400 ppm were tested against sea water stress for their potential effect to drop the harmful effect on cucumber plants. In our results in Table 6; Fig. 4, salinity appeared drop in shoot, root and fresh weight of shoot in cucumber plants but, appeared rose in antioxidant enzymes (peroxidase and polyphenol oxidase), MDA and H_2O_2. Bimetallic NPs at 200 ppm, according to Tukey's test at $P \leq 0.05$, showed significant improvement in shoot, root and fresh weight of shoot compared to salinity groups but, appeared significant decrease in antioxidant enzymes (peroxidase and polyphenol oxidase), MDA and H_2O_2. In this concept on carrot plant where plant morphology, cellular interference, and water balance are all impacted by salt stress at 40 mM and 80 mM., but the most successful treatment for improving the morphological and biochemical parameters was foliar application of MgO-NPs at a dosage of 150 mg/L[58]. Also, MgO NPs can raise the fresh weight in mung beans[59].

Numerous studies have documented the detrimental effects of salinity on growth parameters and biochemical traits. For example, when exposed to 75 mM and 150 mM NaCl, maize seedlings showed the largest decrease in biomass and showed elevated levels of malondialdehyde (MDA), hydrogen peroxide (H_2O_2), total antioxidant capacity (TAC), and polyphenol content[60]. In our results in Table 6, bimetallic ZnO/MgO NPs at 200 ppm showed improvement in shoot, root lengths and fresh weight of shoot by 31.9, 100.1, and 31.01% respectively, but at 400 ppm by 15.3, 50.1 and 27.5% respectively compared to saline groups. The results showed that ZnO/MgO NPs had potential anti-salinity stress activity. It also seemed that the advantageous effects of the bimetallic ZnO/MgO NPs had expanded to reduce the enzyme activities of polyphenol oxidase (PPO) and peroxidase (POD) in both ZnO/MgO NPs groups of cucumber plants compared to saline groups (Fig. 4). Malondialdehyde content (MDA) decreased by 48.09% and 46.19%, respectively, at 200 and 400 ppm in response to ZnO/MgO NPs when compared to the saline group. Also, the contents of H_2O_2 by 28.57% and 31.11%, respectively in Fig. 4. In our study, sea water stress caused high significant increase in peroxidase (POD), polyphenol oxidase (PPO), H_2O_2 and MDA. In parallel with my results Özdamar[61], found that the amount of malondialdehyde (MDA) and CAT

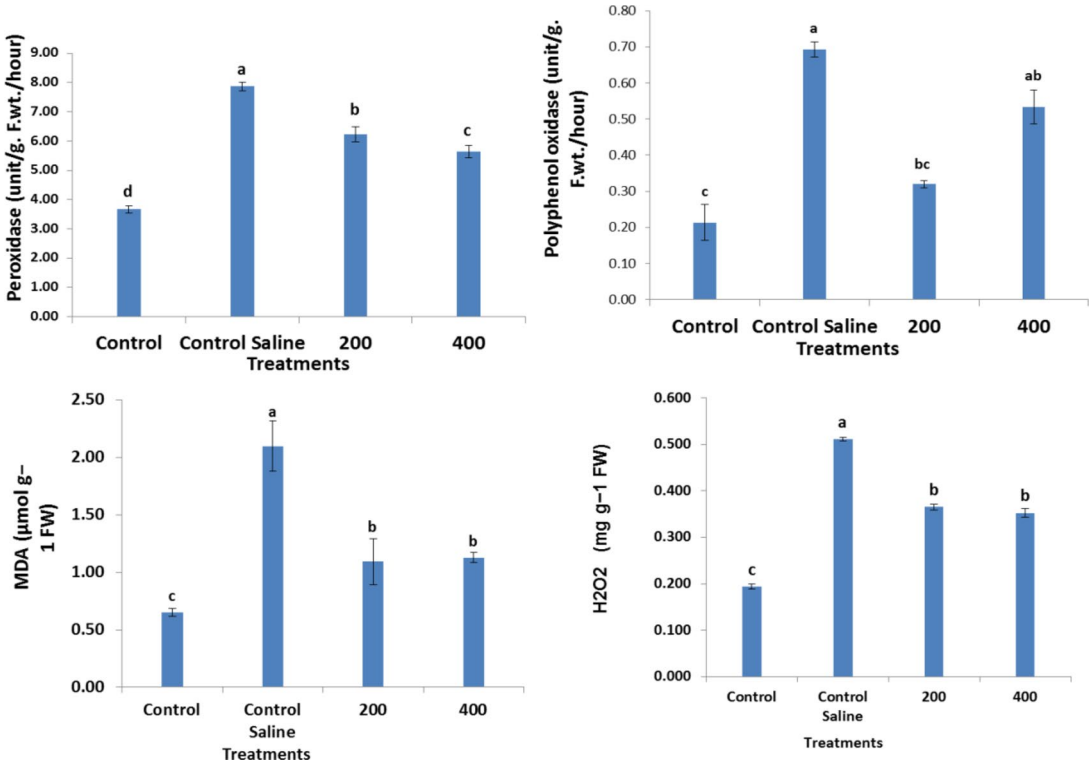

Fig. 4. Cucumber plant peroxidase, polyphenol oxidase, H_2O_2 and MDA contents after various treatments: sea water + ZnO@MgO NPs (200 mg/kg of soil), sea water + ZnO@MgO NPs (400 mg/kg of soil), control saline (irrigation with 35% of sea water), and control (using tap water). The standard deviation of the means plus the mean of three replicates make up each number. Values of the same letter in the same column do not differ significantly; nevertheless, post hoc Tukey's test results at $P < 0.05$ show significant differences between distinct lower-case letters in the same column.

activity rose when eggplant subjected to 100 mM NaCl. The promotion role of ZnO NPS alone, appeared in our previous study[62], which found that ZnO NPs (25, 50, 100 and 200 ppm) have positive effects on carbohydrate, protein, amylase, protease, nitrogen (N), phosphorus (P) and potassium (K) contents of *Phaseolus vulgaris* L. plants. Also, in other study on MgO-NPs at 5, 10, and 20 ppm on *Nigella sativa* appeared enhancement in growth, yield, and metabolic activities[63]. Through increased sucrose synthesis, which in turn biosynthesizes lipopolysaccharides (LP), glycinebetaine (GB), and total soluble protein (TSP), as well as improved ribulose bisphosphate carboxylase-oxygenase activity, photosystem II light-capturing efficiency, and the capacity to transport electrons under salinity stress, ZnO-MgONPs can lessen the negative effects of salinity[64].

There are some others function of bimetallic ZnO/MgO NPs listed in Table 7 also, Fig. 5. illustrate the graphical abstract provided with proper segments of our study. In the future studies we can testing the impacts of bimetallic NPs on a wider range of economic crops, also exploring different bio-synthesis methods, investigating long-term effects on plant health and soil quality.

Conclusion

In summary, the current study portrays a very cost-effective and environmentally responsible technique to biosynthesize of bimetallic ZnO/MgO by using aqueous extracts of *Mentha longifolia* plant without the use of dangerous or poisonous chemicals. The results showed that ZnO/MgO NPs, has antibacterial, antioxidant, and anti-diabetic properties, but MLLE exhibited high inhibition zones in medium inoculated by *E. faecalis*, *E. coli*, *S. typh*, *M. circinelloid C. albicans* and *S. aureus*, respectively. Compared to acarbose, ZnO/MgO NPs exhibited superior activity against α-Amylase inhibition percentage, as evidenced by their IC_{50} value of 117.02 ± 0.56 µg/mL. ZnO/MgO NPs may be employed as a unique approach to boost plant growth of cucumber plants under salinity stress, where growth promotion is needed. Peroxidation of lipid and accumulation of ROS were reduced in cucumber treated with ZnO/MgO NPs. Plants treated with ZnO/MgO NPs showed decreased lipid peroxidation and ROS accumulation. It is indicator the vital role of ZnO/MgO NPs to decrease the harmful effect of salinity on plant. In the future studies, molecular and cytotoxicity studies on plant cell under effect of bimetallic NPs.

Method of synthesis	Application	References
Precipitation method	Anticancer Drug Carrier	65
Green method by *Azadirachta indica*	Wastewater Treatment	66
Green method by *Citrus limonium* fruit juice	Antibacterial activity	67
Precipitation method	Antifungal activity	68
Green method by *Lupinus albus*.	Photocatalytic and Antimicrobial Activities	69
Sol-gel method sol-gel method	Antifungal activity	70
Ethanol–water as a solvent Reflux-assisted co-precipitation technique employing water and ethanol as a solvent	As a catalyst for reactive black 5 dye degradation and p-nitrophenol reduction	71
Green method by oily extract of *Curcuma zedoaria*	Had Leishmanicidal and Anti-Microbial Effects	72
Green method by Rosehip (RH) extract	Antioxidant and anti-inflammatory activity	73
Polymeric ionic liquids	Oxygen reduction reaction and advanced catalysis	74
Facile one-step combustion route	Anti-microbial, cytotoxicity and photocatalysis applications	75
A facile one-pot method	CO_2 adsorption and catalytic conversion	76
Mentha longifolia leaves eques extract	Antibacterial, anti-diabetic, antioxidant agents and plant stimulator for reducing salinity stress	Current study

Table 7. Bimetallic ZnO/MgO nanoparticles' biological activity.

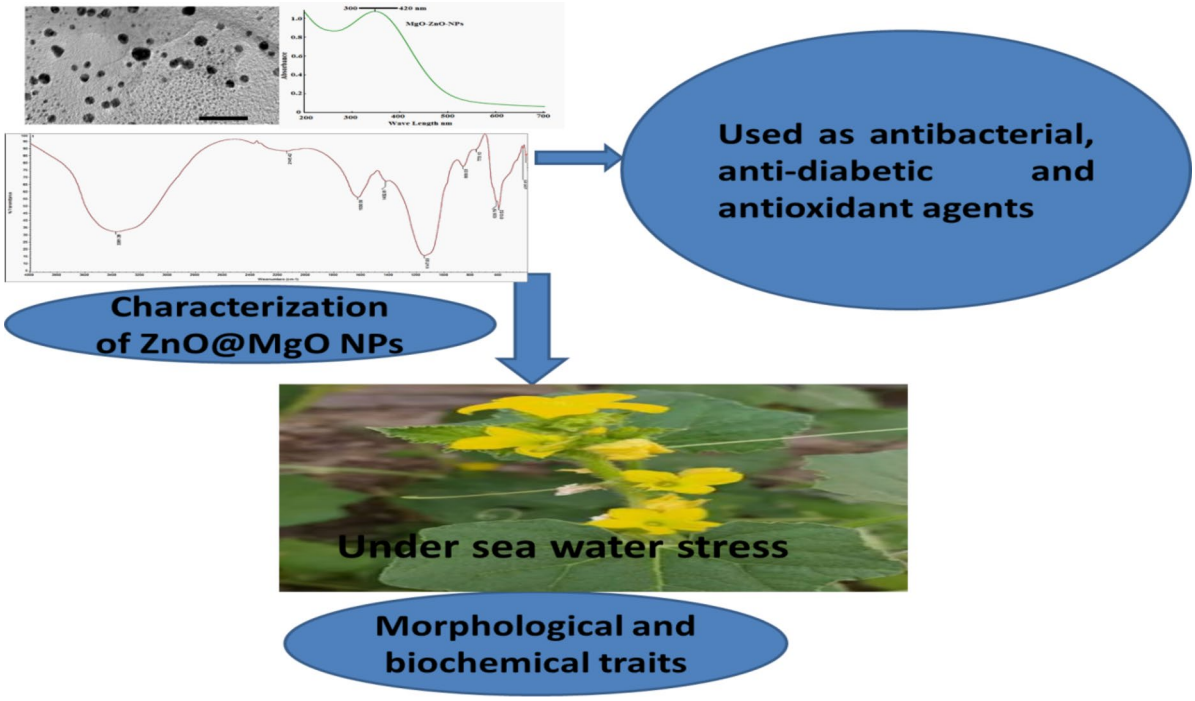

Fig. 5. The graphical abstract of our study, provided with proper segments in the manuscript.

Data availability

All data that support the findings of this study are available within the article.

Received: 6 October 2024; Accepted: 22 January 2025
Published online: 12 February 2025

References

1. Yahya, R. et al. Molecular docking and efficacy of Aloe vera gel based on chitosan NPs against *Helicobacter pylori* and its antioxidant and anti-inflammatory activities. *Polymers* **14**(15), 2994 (2022).
2. Qanash, H. et al. Bioenvironmental applications of myco-created bioactive zinc oxide nanoparticle-doped selenium oxide NPs. *Biomass Convers. Biorefin.*, 1–12 (2023).
3. Al-Rajhi, A. M. & Abdelghany, T. M. Nanoemulsions of some edible oils and their antimicrobial, antioxidant, and anti-hemolytic activities. *BioResources* **18**(1), 1465–1481 (2023).
4. El-Batal, A. I., Ismail, M. A., Amin, M. A., El-Sayyad, G. S. & Osman, M. S. Selenium NPs induce growth and physiological tolerance of wastewater stressed carrot plants. *Biologia* **78**(9), 2339–2355 (2023).

5. Singh, K. et al. Defect and heterostructure engineering assisted S-scheme Nb2O5 nanosystems-based solutions for environmental pollution and energy conversion. *Adv. Colloid Interface Sci.* **332**, 103273 (2024).
6. Abdelghany, T. M. et al. Recent advances in green synthesis of silver NPs and their applications: about future directions. *Rev. BioNanoScience* **8**, 5–16 (2018).
7. Alsalamah, S. A., Alghonaim, M. I., Mohammad, A. M. & Abdel Ghany, T. M. Algal biomass extract as mediator for copper oxide nanoparticle synthesis: applications in control of fungal, bacterial growth, and photocatalytic degradations of dyes. *BioResources* **18**(4), 7474 (2023).
8. Álvarez-Chimal, R. & Arenas-Alatorre, J. Á. Green synthesis of NPs. A biological approach (2023).
9. Batra, V., Kaur, I., Pathania, D. & Chaudhary, V. Efficient dye degradation strategies using green synthesized ZnO-based nanoplatforms: a review. *Appl. Surf. Sci. Adv.* **11**, 100314 (2022).
10. Chaudhary, V. et al. Borophene-based nanomaterials: promising candidates for next-generation gas/vapor chemiresistors. *J. Mater. Sci. Technol.* (2024).
11. Iavicoli, I., Leso, V., Beezhold, D. H. & Shvedova, A. A. Nanotechnology in agriculture: opportunities, toxicological implications, and occupational risks. *Toxicol. Appl. Pharmacol.* **329**, 96–111 (2017).
12. Barsola, B. et al. Exploring bio-nanomaterials as antibiotic allies to combat antimicrobial resistance. *Biofabrication* **16**(4), 042007 (2024).
13. Pathania, D. et al. Essential oil derived biosynthesis of metallic nano-particles: implementations above essence. *Sustain. Mater. Technol.* **30**, e00352 (2021).
14. Chaudhary, V. et al. Biogenic green metal nano systems as efficient anti-cancer agents. *Environ. Res.* **229**, 115933 (2023).
15. Pugazhendhi, A., Prabhu, R., Muruganantham, K., Shanmuganathan, R. & Natarajan, S. Anticancer, antimicrobial and photocatalytic activities of green synthesized magnesium oxide NPs (MgONPs) using aqueous extract of Sargassum Wightii. *J. Photochem. Photobiol. B Biol.* **190**, 86–97 (2019). (2019).
16. Qaddoori, H. T. & Adil, N. The use of Mentha longifolia in the development of some medicines. *Egypt. J. Chem.* **65**(7), 211–219 (2022).
17. Haider, A. J. et al. Characterization of laser dye concentrations in ZnO nanostructures for optimization of random laser emission performance. *Int. J. Mod. Phys. B* **38**(08), 2450111 (2024).
18. Saklani, S. et al. Nanomaterials-integrated electrochemical biosensors as pioneering solutions for zoonotic disease diagnosis. *J. Electrochem. Soc.* **171**(8), 087502 (2024).
19. Seghir, B. B. et al. A., Pohl, P. Exploring the antibacterial potential of green-synthesized MgO and ZnO NPs from two plant root extracts. *Nanomaterials (Basel)* **13**(17), 2425 (2023).
20. Kainat, Khan, M. A. et al. Exploring the therapeutic potential of Hibiscus rosa sinensis synthesized cobalt oxide (Co3O4-NPs) and magnesium oxide NPs (MgO-NPs). *Saudi J. Biol. Sci.* **28**(9), 5157–5167 (2021).
21. Abdelghany, T. M. et al. Phytofabrication of zinc oxide NPs with advanced characterization and its antioxidant, anticancer, and antimicrobial activity against pathogenic microorganisms. *Biomass Convers. Biorefin.* **13**, 417–430 (2023).
22. Acharya, P., Jayaprakasha, G. K., Crosby, K. M., Jifon, J. L. & Patil, B. S. Green-synthesized NPs enhanced seedling growth, yield, and quality of onion (*Allium cepa* L). *ACS Sustain. Chem. Eng.* **7**(17), 14580–14590 (2019).
23. Juárez-Maldonado, A. Impact of nanomaterials on plants: what other implications do they have? *Biocell* **46**(3), 651 (2022).
24. Sharma, P., Ayushi, G., Vineet, K. & Praveen, G. In vitro exposed magnesium oxide NPs enhanced the growth of legume *Macrotyloma uniflorum*. *Environ. Sci. Pollut. Res.*, 1–11 (2022).
25. Gautam, A. et al. Magnesium oxide NPs improved vegetative growth and enhanced productivity, biochemical potency and storage stability of harvested mustard seeds. *Environ. Res.* **229**, 116023 (2023).
26. Ghani, M. I. et al. Foliar application of zinc oxide NPs: an effective strategy to mitigate drought stress in cucumber seedling by modulating antioxidant defense system and osmolytes accumulation. *Chemosphere* **289**, 133202 (2022).
27. Stagnari, F., Onofri, A. & Pisante, M. Response of French bean (*Phaseolus vulgaris* L.) cultivars to foliar applications of magnesium. *Ital. J. Agron.* **4**(3), 101–110 (2009).
28. Kumar, S., Kumar, S. & Mohapatra, T. Interaction between macro-and micro-nutrients in plants. *Front. Plant Sci.* **12**, 665583 (2021).
29. Du, W., Yang, J., Peng, Q., Liang, X. & Mao, H. Comparison study of zinc NPs and zinc sulphate on wheat growth: from toxicity and zinc biofortification. *Chemosphere* **227**, 109–116 (2019).
30. Shams, G., Ranjbar, M. & Amiri, A. Effect of silver NPs on concentration of silver heavy element and growth indexes in cucumber (Cucumis sativus L. negeen). *J. Nanopart. Res.* **15**, 1–12 (2013).
31. Mehmood, S. et al. Alleviation of salt stress in wheat seedlings via multifunctional Bacillus aryabhattai PM34: an in-vitro study. *Sustainability* **13**(14), 8030 (2021).
32. Abdel-Haliem, M. E., Hegazy, H. S., Hassan, N. S. & Naguib, D. M. Effect of silica ions and nano silica on rice plants under salinity stress. *Ecol. Eng.* **99**, 282–289 (2017).
33. Wangsawang, T. et al. A salinity-tolerant japonica cultivar has Na+ exclusion mechanism at leaf sheaths through the function of a na + transporter os HKT 1; 4 under salinity stress. *J. Agron. Crop Sci.* **204**(3), 274–284 (2018).
34. Abdelghany, T. et al. Effect of Thevetia peruviana seeds extract for microbial pathogens and cancer control. *Int. J. Pharmacol.* **17**, 643–655 (2021).
35. French, G. L. Bactericidal agents in the treatment of MRSA infections—the potential role of daptomycin. *J. Antimicrob. Chemother.* **58**, 1107 (2006).
36. Wickramaratne, M. N., Punchihewa, J. C. & Wickramaratne, D. B. M. In-vitro alpha amylase inhibitory activity of the leaf extracts of Adenanthera pavonina. *BMC Complement. Altern. Med.* **16**, 1–5 (2016).
37. Pistia-Brueggeman, G. & Hollingsworth, R. I. A. preparation and screening strategy for glycosidase inhibitors. *Tetrahedron* **57**(42), 8773–8778 (2001).
38. Baliyan, S. et al. Determination of antioxidants by DPPH radical scavenging activity and quantitative phytochemical analysis of Ficus religiosa. *Molecules* **27**(4), 1326 (2022).
39. Lahmass, I. et al. Determination of antioxidant properties of six by-products of *Crocus sativus* L. (saffron) plant products. *Waste Biomass Valor.* **9**, 1349–1357. https://doi.org/10.1007/s12649-017-9851-y (2018).
40. Benzie, I. F. & Strain, J. J. The ferric reducing ability of plasma (FRAP) as a measure of antioxidant power: the FRAP assay. *Anal. Biochem.* **239**, 70–76 (1996).
41. Mukherjee, S. P. & Choudhuri, M. A. Implications of water stressinduced changes in the levels of endogenous ascorbic acid and hydrogen peroxide in Vigna seedlings. *Physiol. Plant.* **58**, 166–170 (1983).
42. Kar, M. & Mishra, D. Catalase, peroxidase, and polyphenoloxidase activities during rice leaf senescence. *Plant. Physiol.* **57**, 315–319. https://doi.org/10.1104/pp.57.2.315 (1976).
43. Bergmeyer, H. U. & Bernt, E. UV-assay with pyruvate and NADH. In *Methods of Enzymatic Analysis* 574–579 (Academic, 1974).
44. Tsikas, D. Assessment of lipid peroxidation by measuring malondialdehyde (MDA) and relatives in biological samples: Analytical and biological challenges. *Anal. Biochem.* **524**, 13–30 (2017).
45. Sergiev, I., Alexieva, V. & Karanov, E. Effect of spermine, atrazine and combination between them on some endogenous protective systems and stress markers in plants. *Compt. Rend. Acad. Bulg. Sci.* **51**(3), 121–124 (1997).
46. Iribarnegaray, V. et al. Magnesium-doped zinc oxide NPs alter biofilm formation of *Proteus mirabilis*. *Nanomedicine* **14**(12), 1551–1564 (2019).

47. Zamiri, R., Kaushal, A., Rebelo, A. & Ferreira, J. M. F. Er doped ZnO nanoplates: synthesis, optical and dielectric properties. *Ceram. Int.* **40**(1), 1635–1639 (2014).
48. Essien, S. O., Young, B. & Baroutian, S. Recent advances in subcritical water and supercritical carbon dioxide extraction of bioactive compounds from plant materials. *Trends Food Sci. Technol.* **97**, 156–169 (2020).
49. Ogunyemi, S. O. et al. The bio-synthesis of three metal oxide NPs (ZnO, MnO2, and MgO) and their antibacterial activity against the bacterial leaf blight pathogen. *Front. Microbiol.* **11**, 588326 (2020).
50. Taha, B. A., Mehde, M. S., Haider, A. J. & Arsad, N. Mathematical model of the DBR laser for thermal tuning: taxonomy and performance effectiveness with PbSe materials. *J. Opt.* **52**(3), 1415–1425 (2023).
51. Taha, B. A. et al. Plasmonic-enabled nanostructures for designing the next generation of silicon photodetectors: trends, engineering and opportunities. *Surf. Interfaces*, 104334 (2024).
52. Al-Rajhi, A. M. H. et al. In situ green synthesis of Cu-doped ZnO based polymers nanocomposite with studying antimicrobial, antioxidant and anti-inflammatory activities. *Appl. Biol. Chem.* **65**, 35 (2022).
53. Al-Rajhi, A. M. H. et al. Molecular interaction studies and phytochemical characterization of *Mentha pulegium* L. constituents with multiple biological utilities as antioxidant, antimicrobial, anticancer and anti-hemolytic agents. *Molecules* **27**(15), 4824 (2022).
54. Ceyhan-Güvensen, N. & Keskin, D. Chemical content and antimicrobial properties of three different extracts of Mentha pulegium leaves from Mugla Region. *Turk. J. Environ. Biol.* **37**, 1341–1346 (2016).
55. Baali, F. et al. Wound-healing activity of Algerian *Lavandula stoechas* and *Mentha pulegium* extracts: from traditional use to scientific validation. *Plant. Biosyst. Int. J. Deal All Asp. Plant. Biol.* **156**, 427–439 (2021).
56. Rudayni, H. A. et al. Synthesis and biological activity evaluations of green ZnO-decorated acid-activated bentonite-mediated curcumin extract (ZnO/CU/BE) as antioxidant and antidiabetic agents. *J. Funct. Biomater.* **14**(4), 198 (2023).
57. El-Badri, A. M. et al. Selenium and zinc oxide NPs modulate the molecular and morpho-physiological processes during seed germination of Brassica napus under salt stress. *Ecotoxicol. Environ. Saf.* **225**, 112695 (2021).
58. Mirrani, H. M. et al. Magnesium NPs extirpate salt stress in carrots (*Daucus carota* L.) through metabolomics regulations. *Plant. Physiol. Biochem.* **207**, 108383 (2024).
59. Mahawar, H. et al. Deciphering the mode of interactions of NPs with mung bean (*Vigna radiata* L.). Isr. *J. Plant. Sci.* **65**(1–2), 74–82 (2018).
60. AbdElgawad, H. et al. High salinity induces different oxidative stress and antioxidant responses in maize seedlings organs. *Front. Plant Sci.* **7**, 276 (2016).
61. Özdamar, F. Ö., Furtana, G. B., Tıpırdamaz, R. & Duman, H. H2O2 and NO mitigate salt stress by regulating antioxidant enzymes in in two eggplant (*Solanum melongena* L.) genotypes. *Soil Stud.* **11**(1), 1–6 (2022).
62. Amin, M. A. & Badawy, A. A. Metabolic changes in common bean plants in response to zinc NPs and zinc sulfate. *Int. J. Innov. Sci. Eng. Technol.* **4**, 321–335 (2017).
63. Amin, M. A. A. et al. Green synthesis of magnesium oxide NPs using endophytic fungal strain to improve the growth, metabolic activities, yield traits, and phenolic compounds content of *Nigella sativa* L. *Green. Process. Synth.* **13**(1), 20230215 (2024).
64. Seleiman, M. F. et al. Zinc oxide NPs: a unique saline stress mitigator with the potential to increase future crop production. *South Afr. J. Bot.* **159**, 208–218 (2023).
65. Kumar, R. et al. Can be a bimetal oxide ZnO–MgO NPs anticancer drug carrier and deliver? Doxorubicin adsorption/release study. *J. Nanosci. Nanotechnol.* **15**(2), 1543–1553 (2015).
66. Yadav, K. S. K. & Manikandan, S. Green synthesized mixed oxides (ZnO and MgO) NPs for wastewater treatment over filtration technique for bioremediation application: a comparative study. *J. Surv. Fish. Sci.* **10** (1S), 787–794 (2023).
67. Priyadharshini, S. et al. A cleaner and multifunctional Citrus limonium-assisted ZnO/MgO nanocomposite synthesis: extensive investigations on antibacterial, antioxidant, and antidiabetic applications. *Mater. Today Commun.* **41**, 110620 (2024).
68. Ismail, A. M., El-Gawad, A. & Mona, E. Antifungal activity of MgO and ZnO NPs against powdery mildew of pepper under greenhouse conditions. *Egypt. J. Agric. Res.* **99**(4), 421–434 (2021).
69. Muhammed, A., Asere, T. G. & Diriba, T. F. Photocatalytic and antimicrobial properties of ZnO and Mg-doped ZnO NPs synthesized using Lupinus albus leaf. extract. *ACS Omega* **9**(2), 2480–2490. https://doi.org/10.1021/acsomega.3c07093 (2024).
70. Sierra-Fernandez, A. et al. Synthesis, photocatalytic, and antifungal properties of MgO, ZnO and Zn/Mg oxide NPs for the protection of calcareous stone heritage. *ACS Appl. Mater. Interfaces* **9**(29), 24873–24886 (2017).
71. Khan, S. R. et al. Synthesis and characterization of Mg–Zn bimetallic NPs: selective hydrogenation of p-nitrophenol, degradation of reactive carbon black 5 and fuel additive. *J. Inorg. Organomet. Polym. Mater.* **30**, 438–450 (2020).
72. Sheema, Akbar, S., Jamal, Q. & Zafar, S. Leishmanicidal and anti-microbial effects of MgO–ZnO bimetallic nanocomposites, fabricated with Curcuma zedoaria oil. *J. Inorg. Organomet. Polym. Mater.*, 1–12 (2024).
73. Martin, V. et al. Green synthesis of Zn–Mg layered hydroxide NPs with surface-mediated antioxidant and anti-inflammatory activity. *Surf. Interfaces* **46**, 104037 (2024).
74. Liu, M., Zhang, J., Peng, Y. & Guan, S. Synergistic dual sites of Zn–Mg on hierarchical porous carbon as an advanced oxygen reduction electrocatalyst for Zn–air batteries. *Dalton Trans.* **53**(21), 8940–8947 (2024).
75. Hamdy, M. S. et al. Novel Mg/ ZnO NPs synthesized by facile one-step combustion route for anti-microbial, cytotoxicity and photocatalysis applications. *J. Nanostruct. Chem.* **11**, 147–163 (2021).
76. Gao, Z., Liang, L., Zhang, X., Xu, P. & Sun, J. Facile one-pot synthesis of Zn/Mg-MOF-74 with unsaturated coordination metal centers for efficient CO2 adsorption and conversion to cyclic carbonates. *ACS Appl. Mater. Interfaces*. **13**(51), 61334–61345 (2021).

Acknowledgements

The authors gratefully acknowledge the technical and financial support provided by Jouf University, University of Jeddah, and King Abdulaziz University, Saudi Arabia.

Author contributions

Author Contributions: Investigation and formal analysis S.S., M.S.A., M.H.A. and M.K.T.; Methodology, Resources, Writing – review and editing, A.A.S., M.Y.M.E., M.A.A. and S.K.A. All authors have approved to publish the paper.

Funding

Not applicable.

Declarations

Competing interests

The authors declare no competing interests.

Additional information

Correspondence and requests for materials should be addressed to S.S. or M.A.A.

Reprints and permissions information is available at www.nature.com/reprints.

Publisher's note Springer Nature remains neutral with regard to jurisdictional claims in published maps and institutional affiliations.